Coastal River Response to Transgression: A New Look at the Trinity Incised Valley Using Multi-Resolution Seismic Imaging

John M. Swartz*[1,2,3], Patricia Standring[2,3], John Goff[3], Sean Gulick[2,3], Chris Lowery[3]

1- The Water Institute of the Gulf

2- Department of Geological Sciences, The University of Texas at Austin

3- Institute for Geophysics, The University of Texas at Austin

*jswartz@thewaterinstitute.org

@littlebiggeo

@orbulinasdad

@patty_standring

THIS MANUSCRIPT HAS NOT COMPLETED THE PEER-REVIEW PROCESS

ABSTRACT

Modern lowland river systems show transitions in flow characteristics near coastlines that lead to systematic changes in sediment deposition and stratigraphic architecture. Sensitivity of fluvial morphodynamics to base-level has important implications for the prediction and interpretation of fluvial stratigraphy, particularly in deposits formed during periods of relative sea-level rise such as the early Holocene. Improving our understanding of how fluvial stratigraphy is created and preserved in such environments is crucial to paleoenvironmental reconstruction, sand resource estimation, and mapping subsurface facies distributions. A significant challenge has been capturing the spatiotemporal evolution of such systems on long timescales (centuries to millennia), often due to poor data coverage and resolution. Here we investigate the offshore stratigraphic architecture of the Trinity coastal river system, Texas. The paleo-valley is interpreted to have formed during the last lowstand and filled by backstepping fluvial-deltaic and estuarine sediments

over the Holocene. However, the nature of this transition and resulting stratigraphy is unclear. We present unprecedented imaging of the incised valley and fluvial stratigraphy using a combination of over 500km^2 of 3D seismic and nearly 700km of full waveform chirp data with 250m line spacing, combined with sediment cores and geotechnical borings. Our chirp processing technique creates images of strata on the decimeter scale, allowing for near outcrop scale mapping and interpretation. Archival industry 3D seismic data show that the basal valley fill is comprised of a highly-amalgamated fluvial channel belt with numerous avulsions and loop cutoffs. The chirp data show the transition of individual fluvial channels from sand rich, laterally migrating systems to muddy channels that depict high rates of vertical aggradation and little lateral movement. We observe the interaction of these channels with the paleo-floodplain and show that aggradation and infilling of the incised valley is dominated by fluvial processes before a transition to bay and estuarine conditions. Our work illustrates that traditional models of incised valley filling and fluvial response to transgression fail to fully capture the morphodynamics of coastal river systems.

INTRODUCTION

Alluvial rivers are dynamic sedimentary systems that adjust to external forcings and internal processes in ways that are not completely understood. In particular, how fluvial morphodynamics and sedimentation respond to base-level rise is an important topic for both predicting evolution of coastal systems under rising seas as well as interpreting the rock record (e.g., Blum and Tornqvist, 2000; Cattaneo and Steel, 2002; Jerolmack, 2009; Miall 2014). Some of the most complete records of fluvial and coastal evolution during periods of sea-level fall and rise are found in incised valleys: stratigraphic features generated by fluvial incision and commonly filled by transgressive fluvio-deltaic and coastal deposition (e.g., Anderson et al., 2014; Reijenstein et al., 2011; Nordfjord et al., 2005; Zaitlin et al., 1994). Study of the Holocene fluvial record has

helped develop commonly-applied models of river and delta transgression and back-stepping, in part due to the comparatively well-constrained rates of relative sea-level rise in this period (Anderson et al., 2016; Milliken et al., 2008; Moran et al., 2017). Additionally, sedimentary deposits of these Holocene rivers have recently come under increasing focus as potential sources of large quantities of sand and other sediments useful to coastal nourishment and resiliency projects as traditional sources disappear (e.g.,; Sutherland et al., 2017; Torres et al., 2017). The study of these Holocene systems therefore can help address both coastal evolution and fluvial dynamics in the face of increasing rates of sea-level rise while also unlocking the potential of their stratigraphy to aid in coastal restoration.

Lowland rivers experience a transition from uniform to varying flow conditions, or a backwater, as they approach the coast (e.g., Chatanantavet et al., 2012; Hoyal and Sheets, 2009; Lamb et al., 2012). On the modern Trinity River this interval is correlated with significant changes in geomorphology and sediment transport, including decreased lateral migration rates, downstream sediment fining, and a reduction in point bar area (Smith and Mohrig, 2017; Mason and Mohrig, 2018). Similar behavior is observed in a number of other alluvial rivers, including the Mississippi (Hudson and Kesel, 2000; Nittrouer et al., 2012). The onset of backwater hydraulics has also been proposed as a primary control on the location of distributary channel avulsions and thus predict overall patterns of fluvial-deltaic deposition (e.g., Ganti et al., 2014; Jerolmack and Swenson, 2007; Moodie et al., 2019; Zheng et al., 2019). While many studies have shown the link between in-channel fluvial aggradation and base-level rise, the details of how the overall fluvial system adjusts are less clear (e.g., Mackin, 1948; Leopold and Bull, 1979). Due to the link between fluvial morphodynamics and the backwater zone, which is in turn a function of distance to the river mouth, an expectation emerges that fluvial systems should not simply aggrade, back-step and transgress, while maintaining constant morphology and dynamics. Rather these systems undergo a change in

sediment transport and resulting geomorphology that leads to different depositional architecture (e.g., Fernandes et al., 2016; Moran et al., 2017; Trower et al., 2018).

To provide a more detailed characterization of the morphologic changes associated with the fluvial to deltaic transition, we focus on the Trinity incised valley offshore east Texas in the Gulf of Mexico (Figure 1; Anderson et al., 2016). This system has a well-developed stratigraphic framework that provides detailed characterization of lithology, age, and depositional paleoenvironments. However, earlier geophysical methodologies lacked the necessary resolution to accurately characterize the fine-scale stratigraphic architecture of the observed transitions and fully capture the adjustment and evolution of the fluvial system during relative sea-level rise (Thomas and Anderson, 2004). Here we revisit the Trinity incised valley and use a dense survey grid of high-resolution chirp reflection data, 3D seismic imaging, cores and digitized archival lithologic records. Using these data, we investigate the shallow stratigraphy corresponding with the Holocene transgression and delineate several seismic units corresponding with periods of dominantly fluvial, deltaic, and estuarine deposition. We also detail the potential paleogeomorphology of the Trinity valley using 3D seismic surface extractions. This work demonstrates the evolution of the paleo-Trinity river from a laterally migrating meandering system that formed the incised valley to a system dominated by vertical aggradation and floodplain building as the system transitioned from terrestrial to more estuary-like conditions in the face of environmental change. Finally, we examine these transitions in the context of the geomorphic adjustment of fluvial systems to base-level. Additional papers from this project explore the estuarine section's stratigraphic (Burstein et al., 2021) and paleoenvironmental (Standring et al., 2021) evolution in detail.

STUDY AREA

The Trinity incised valley has been the focus of significant research over the past several decades, and as a result detailed maps and models of the valley sedimentary architecture and

patterns and timing of shifts in depositional environment have been created primarily using geotechnical borings, sediment cores, and seismic datasets of varied frequency and resolution (e.g., Thomas and Anderson, 1994; Rodriguez et al., 2005; Anderson et al., 2008; Figure 1). The majority of this work has focused on understanding the overall evolution of the Trinity valley and surrounding east Texas continental shelf from previous sea-level highstands to the present (Anderson et al., 2016). The Trinity incised valley began forming during sea-level fall from marine isotope stage (MIS) 5-3 wherein it extended from the modern-day Galveston Bay across the continental shelf (Thomas and Anderson, 1994; Figure 2). It reached its maximum shelf edge location during the last lowstand (MIS 2) at 22-17 ka before present and the associated erosion produced a significant, regionally correlatable erosional surface (Simms et al., 2007). Total relief of the valley surface has been measured at 30-40 m across the shelf, although due to subsequent infilling it only exists offshore as a stratigraphic feature entirely buried beneath the modern seafloor (Thomas and Anderson, 1994).

Sea-level rise following the MIS2 low-stand triggered aggradation and valley filling across the continental shelf for the Trinity and other Gulf of Mexico fluvial systems (Anderson et al., 2016). Despite the rapid rates of sea level rise between ~17 ka and ~10 ka the Trinity system maintained a shelf-edge delta until at least ~14 ka before beginning to transgress towards its modern position (Wellner et al., 2004). The record of Holocene sea level rise in the Gulf of Mexico is relatively well constrained, and captures the transition from relatively rapid rates of 4.2 mm/yr from 12 ka to 1.4 mm/yr at 7.9 ka (Milliken et al., 2008; Figure 2). From ~10 ka onward The Trinity valley was filled by a series of landward stepping transgressive depositional packages interpreted as successions of fluvial, deltaic, bay, and tidal deposits (Rodriguez et al., 2005; Thomas and Anderson, 1994; Figure 3). The relatively rapid transition from fluvial deposition to

deltaic and estuarine, as well as the back-stepping nature of the deposits towards the modern Trinity delta, has been interpreted as due to the episodic nature of early Holocene sea level rise, or alternatively due to differential flooding of antecedent topography (Anderson et al., 2008; Rodriguez et al., 2005; Simms and Rodriguez, 2014; Thomas and Anderson, 1994; Figure 2a). Additionally, the pattern of back-stepping as well as the presence of the modern Galveston Bay throughout the Holocene implies that sediment supply of the Holocene Trinity River was unable to keep up with rates of base-level rise, in contrast to several other Gulf of Mexico rivers (Simms et al., 2006; Anderson et al., 2016).

The stratigraphic architecture of the Trinity valley has been previously interpreted on a broad scale through a combination of cores and geophysical data (Figure 3; Anderson et al., 2016; Rodriguez et al., 2005; Thomas and Anderson, 1994). The following framework is that built by Thomas (1991). The broad erosional valley base in the study area is located ~30m below the modern seafloor, and is immediately overlain by a 10-15m thick package of gravels, sands, interbedded silts and clays as well as dense peats and vegetation lenses. This basal unit has been interpreted to represent an amalgamated package of fluvial sands and floodplain sediments deposited during the early Holocene transgression, with some radiocarbon dating indicating the upper portions were deposited as recently as 10.3 kyr before present. Thomas (1991) also noted that the top of this unit is commonly associated with seismic blanking and little acoustic penetration which is a potential signature of coarse grained material and/or shallow biogenic gas accumulation along lithologic contacts. Above this unit is a 5-15m section of interbedded sand, mud, and silt that micropaleontological analyses indicates is comprised of floodplain, deltaic and upper bay sediments, with deposition occurring between 8-10 ka before present. The final unit sees a transition to more open bay or estuarine conditions, and in portions of the study area significant scours associated with flood-tide delta deposits (Anderson et al., 2016; Thomas, 1991). Thomas and Anderson (1994) proposed this succession of units as representative of the overall transgressive sequence, with relatively constant fluvial conditions and backstepping driven by relative sea-level rise rather than aggradation or changes in fluvial dynamics (Figure 3).

METHODS

We primarily use acoustic chirp subbottom and 3D seismic data in this study. Over ~1000 km of 2D chirp have been collected by the University of Texas Institute for Geophysics (UTIG) over the eastern Gulf of Mexico shelf as part of ongoing sand resource assessment work for the Bureaus of Ocean and Energy Management (BOEM) as well as summer field courses (Figure 4). The main survey consists of 45 15-km long, parallel lines oriented perpendicular to modern seafloor dip and spaced at 200-300m intervals, forming a survey area of ~175 km^2 (Figure 4). Chirp data were collected using an Edgetech 512i sub-bottom profiler, configured with a 20ms, 0.7-12 kHz swept-frequency pulse. The full-waveform output was recorded for each survey, which allows for wavelet-based (seismic) processing and maximum sub-surface resolution (Goff et al., 2015). These full waveform chirp data were processed using Paradigm Echos and the workflow included tide and tow depth corrections, secondary deconvolution, heave removal, and trace equalization (Saustrup et al., 2019). This workflow provides both a high-resolution, full waveform dataset that can be interpreted at nearly decimeter scale resolution, as well as a more conventional envelope dataset which in this case has benefitted from seismic processing steps above and is useful for more regional interpretations (Saustrup et al., 2019; Figure 5). An additional ~250 km of chirp lines collected by Texas A&M Galveston (TAMUG) and the U.S. Geological Survey (USGS) within the study area were obtained and the chirp datasets partially re-processed, although due to the lack of the original raw output only the re-processed envelope chirp are available. Seismic stratigraphic interpretations were performed using Petrel 2016 and Landmark DecisionSpace Desktop. Chirp interpretation relied on the recognition of distinct seismic horizons that either act as regional unconformities and/or conformable surfaces that separate seismic units: packages of reflectors that represent related stratigraphy (Reijenstein et al., 2011). When appropriate, approximate depths and thicknesses were converted from two-way travel time in

milliseconds to meters using an average velocity of 1525 m/s (Abdulah et al., 2004). Interpretation of environment and depositional processes within each unit relies on identification of smaller scale geometries, amplitudes, and reflector continuity (e.g., Liu et al., 2017; Reijenstein et al., 2011).

Seismic surveys collected in the Gulf of Mexico by the energy industry enter the public domain following a 25-year exclusive window. Recently, sets of early 3D surveys on the continental shelf have begun to be publicly released by the BOEM and the USGS. A 3D seismic survey, B-12-93-TX, collected by Shell Offshore in 1993 has a 750 km^2 footprint covering a significant portion of the study area (Figure 4). This survey was acquired with a 30m line spacing, 30m common depth point (CDP) spacing, and a 4ms sampling interval. The resulting data were processed and time migrated, although details of this processing are not available. The average frequency content of the survey within the upper 100ms is approximately 25 Hz (Figures 5, 6). The survey was imported into Petrel 2016 and a crossline filter of 90m (or three lines) applied to the data volume. This smooths, but does not eliminate, striping artifacts present within the upper 500ms of the data volume that are a result of the acquisition footprint.

Seismic morphology of the Trinity incised valley was analyzed by identification and mapping of a shallow, regionally conformable horizon located between 40-60 ms and the computation of trace attributes (Figure 6). This value was chosen based on published values of the depth to the valley bottom as well as the approximate depth of the basal layer present within our chirp stratigraphy (Figure 6; Thomas and Anderson, 1994). The low frequency content of the survey means that any single wavelet, or reflector, is over 20ms thick (Figures 5, 6). We map the upper portion of the reflector throughout the entire volume and then calculate a 20ms envelope median coherency along this horizon. This attribute enhances trace discontinuity present within a given window, and as applied here helps identify anomalous amplitudes that often correspond to

channel bodies and other geomorphic elements (e.g., Calves et al., 2008; Reijenstein et al., 2011). The resulting image allows for qualitative analysis of morphology present within the mapped interval (Figure 7). Due to the low 3D seismic frequency, combined with the chosen time envelope, the resulting image is likely amalgamating a significant amount of vertical stratigraphy and is not a snap-shot of a true geomorphic surface but rather a time-transgressive representation of the unit stratigraphy.

As part of a broader and ongoing BOEM-funded project assessing sand resources throughout the Gulf of Mexico all potential geological records such as cores, geotechnical surveys, shallow boreholes, and other potential datasets have been located, digitized, and archived. These include most of the original cores and geotechnical borings used in initial studies of Trinity incised valley, and notably include several that penetrate tens of meters through the base of the incised valley as well as provide radiocarbon age control for several key intervals (Rodriguez et al., 2005; Thomas and Anderson, 1994). We additionally collected a number of piston cores ranging from 2-6 m in penetration that help constrain the uppermost shelf stratigraphy (Figure 4). These geologic records are used to help constrain lithology, depositional environment, and potential depositional age.

RESULTS AND INTERPRETATION

Three regionally extensive surfaces (H1-H3) were identified and mapped throughout the Trinity incised valley stratigraphy (Figures 8-13). These surfaces were tied to available piston core and platform borings that provide lithology and paleo-environmental interpretation. These surfaces are found to correlate to previously identified and interpreted contacts between dominantly fluvial, deltaic, and estuarine depositional units (Thomas and Anderson, 1994).

Horizon H4 is observed only along the edges of the valley and is a steep unconformity that truncates layers outside the valley, whereas internal valley stratigraphy onlaps onto the horizon (Figures 8, 10). This horizon corresponds to the erosional unconformity defining the overall extent of the Trinity incised valley, although its base is not observable within the chirp dataset (Thomas, 1991; Rodriguez et al., 2005). The lowermost valley surface, horizon H3, is a varying amplitude reflector that commonly separates low-amplitude laminated seismic facies above from high-amplitude laterally accreting and chaotic reflectors or complete acoustic blanking below (Figures 8, 10, 12). For the majority of the study area, H3 forms a sharp acoustic contact, and the observed masking is characteristic of biogenic gas accumulation along a lithologic contact as observed previously within the Trinity valley and elsewhere (e.g., Rodriguez et al., 2005; Thomas and Anderson, 1994; Garcia-Gil et al., 2002). Where this acoustic blanking is not present lateral accretion surfaces and potential channel forms are observed. Based on its' depth and acoustic character H3 corresponds to the previously interpreted contact between coarse grained amalgamated fluvial sediments deposited during the low-stand and early transgression and initial deltaic deposition (Thomas and Anderson, 1994). H3 is consistently found at depths of 15-20 ms (12-16 m) below the seafloor across most of the study area, and locally shallows to depths of 5-8 ms (3-6 m) (Figure 14).

Coring through these shallow intervals revealed that the acoustic contact is related to a sharp transition between silty, sandy clays and very fine sands with trace deltaic or upper bay microfossils to barren well-sorted, oxidized sands (Figure 14). Additionally, in the lower valley H3 correlates with the previously interpreted boundary between floodplain deposits and delta sediments (Figure 15; Thomas and Anderson, 1994). The base of the valley is located ~10-15 m (~7-12 ms) below H3 and is not observed in the chirp data (Figures 8, 10, 12). The acoustic

character and correlation to the lithologic contact between potential fluvial material and delta deposits indicate that surface H3 represents the top of the amalgamated fluvial section. A structure map of H3 shows the presence of numerous deep and sinuous channel forms, lending support to the interpretation of H3 as a fluvial surface (Figure 16). The shallower intervals of H3 likely correspond to fluvial terraces previously observed within both offshore stratigraphy as well as in the modern Trinity River valley. This interpretation is supported by the lithology encountered in Piston Core 2 (PC-2) (Figure 14; Morton et al., 1996; Blum and Price, 1998; Rodriguez et al., 2005).

Horizon H2 is a varying amplitude reflector that separates low amplitude laminated seismic facies below from higher amplitude laminated facies above (Figures 8, 10, 12). H2 varies between 25 and 50 ms depth and is generally deeper to the south while shallowing along the valley edges and to the north (Figure 16). In the northern part of the study area, H2 appears sub-parallel and conformable with layers above and below, but towards the south it appears as a sharp unconformity significantly truncating lower stratigraphy while being alternatively draped or overlain by onlapping strata (Figures 8, 10, 12). Cores of these sediments consisted of very fine to fine sands, organic rich clays, and fine interbedded sandy clays with significant wood fragments and plant debris, whereas above horizon H2 there is a transition to more silty and sandy clays and less plant matter (Figures 14, 15; Thomas, 1991). The sediments below H2 were deposited in a deltaic or upper-bay environment, whereas above H2 there is a transition to middle bay or open estuarine conditions with less terrestrial input, according to paleo-environmental analysis of foraminiferal abundances (Thomas, 1991). The shallowest horizon, H1, is the modern seafloor (Figures 8, 10, 12). H1 varies between 20 and 25 ms depth, with a general dip to the southwest (Figure 16). Between H1 and H2 layers are typically sub-parallel and laminated in the northern portion of the

valley, while to the south more onlapping configurations are observed (Figures 12, 13). The upper stratigraphic interval also includes widespread high-amplitude rugose or corrugated reflectors that appear to be small scale, low relief channel forms (Figures 8, 10, 12). The stratigraphy between H1 and H2 corresponds with the middle-bay or estuarine unit defined by Thomas (1991) and Rodriguez et al. (2005).

Together these horizons define the observed seismic units: U3 is the unit of fluvial deposition between H3 and H4, U2 is the deltaic unit between H2 and H3, and U1 is the final estuarine unit between H1 and H2 (Figures 16, 17). U1 is on average 10 ms, or ~7 meters, thick, but increases substantially to the south to 20 ms, or ~15 meters, corresponding with the deepest apparent erosion associated with H2 of the underlying strata (Figures 12, 16, 17). U2 is also 10 ms thick on average, but the pattern of deposition differs from U1. The thickest regions of U2 appear to correlate with the deepest portions of H3, or the top of the fluvial section (Figures 16, 17).

DISCUSSION

The characteristic backstepping stratigraphic architecture of fluvial, deltaic, and estuarine sediments within the Trinity incised valley have formed the basis of conceptual models of alluvial river response to relative sea level rise (e.g., Blum and Tornqvist, 2000; Anderson et al., 2016). The specific fluvial sedimentation patterns that occur during an overall period of transgression are not as well constrained as the broader spatial patterns, however. Earlier interpretation of the Trinity valley stratigraphy implicitly included assumptions of relatively invariant fluvial form and morphodynamics along the entirety of the coastal reach, and that fluvial channels with insufficient sediment supply would be “flooded” by transgression and the resulting relict topography covered by more deltaic or estuarine sediments separated by a distinct flooding surface (e.g., Pearson et al.,

1986; Thomas and Anderson, 1994; Zaitlin et al., 1994). In-channel aggradation because of base-level rise was held to be geologically instantaneous and would be overwhelmed by sufficient rates of relative sea-level rise (Thomas, 1991). We test these earlier interpretations using more advanced geophysical imaging techniques and place them in the context of recent advances in understanding of fluvial morphodynamic adjustment (e.g., Lentsch et al., 2009; Martin et al., 2009; Moran et al., 2017). We observe a broadly similar set of depositional units as in previous work but with significant differences in the internal architecture and associated formational processes.

While the exact basal valley surface is hard to observe within either our 3D seismic dataset or the high-resolution chirp reflection data, the edges and overall valley extent are well-defined (Figures 7, 8, 10). Earlier work proposed that the lowermost unit contained within the valley corresponds to fluvial sediments deposited within the early to middle Holocene but lacked the necessary line density or resolution to observe specific morphological elements corresponding to the paleo-Trinity River (Thomas and Anderson, 1994; Rodriguez et al., 2005). Qualitative geomorphic interpretation of the 3D seismic interval associated with this fluvial unit shows the presence of numerous sinuous channel forms, lateral accretion surfaces forming potential point bar deposits, and shallow terraces (Figure 7). These elements are similar to those observed within modern alluvial river valleys including the Trinity as well as other incised valley systems investigated using 3D seismic (e.g., Morton et al., 1996; Reijenstein et al., 2011; Durkin et al., 2017). The overall valley extent appears to coincide with the maximum extent of the basal meander belt (Figures 7, 8, 10). This relationship potentially indicates that a large proportion of the overall valley stratigraphic form was created during the early Holocene transgression, rather than the period of downcutting and erosion during earlier sea-level fall (Anderson et al., 2016). The overall thickness of this unit as observed within cores and platform borings is on average 12 meters

(Thomas and Anderson, 1994). This thickness is over twice the formational flow depth of the Trinity River and has been used to interpret the basal fluvial unit as representing a period of significant reworking and amalgamation due to avulsion and reworking by lateral migration (Moran et al., 2017). The variable acoustic facies of the fluvial unit, seismic morphology, and presence of a high percentage of sands and interbedded organic rich material support the interpretation of this unit as an amalgamated channel belt (e.g., Gibling, 2006). The total channel belt width varies between 6-10 km whereas the observed channel width of the paleo-Trinity within the chirp and 3D seismic is on roughly 100-200m leading to channel belt width to channel width ratios of 25-50. These ratios are higher are than observed in other preserved and modern systems (e.g., Karssenberg and Bridge, 2008; Fernandes et al., 2016). The overall thickness of this basal unit has been interpreted as representing the total amount of Holocene fluvial aggradation within the valley before continued transgression (Thomas and Anderson, 1994; Moran et al., 2017).

Earlier work identified a flooding surface at the top of the basal channel belt marking the transition from fluvial to bay and deltaic conditions (Thomas and Anderson, 1994; Rodriguez et al., 2005). We do not observe such a sharp transition. Rather, the transition from fluvial to deltaic appears to coincide with a significant adjustment in channel behavior of the paleo-Trinity. While the basal channel belt is time-transgressive and consists of numerous channel avulsions and reworked fluvial deposits, a potential “last” channel can be observed within the chirp structure map of horizon H3 (Figure 16). This channel likely corresponds to the position of the Trinity River at the fluvio-deltaic transition. Although the lines are separated by 200-300m, a sinuous course of this channel is present roughly 5-10 ms deeper than the surrounding surface, which corresponds with one of the observed channel forms identified within the 3D seismic extract (Figures 7, 17). The channel form appears to have been created during the period of lateral migration and avulsion

that deposited the broader channel belt. However, rather than being filled by channel abandonment facies or reworked as observed elsewhere in the system, it instead appears to play a key role in subsequent deltaic deposition. In the shallow portion of the valley, the channel form propagates upward maintaining 2-5m of relief (Figure 18). Reflectors originating from the edges of the channel appear to downlap on the surrounding paleo-floodplain, suggesting continued levee and floodplain growth sourced from the channel during this overall period of aggradation (Figures 17, 18). This transition in geometry and channel behavior is associated with a shift from coarse grained deposition to fine grained organic rich clays and silts which corresponds with the observed change in seismic facies (Figure 15; Thomas, 1991). This change from a system dominated by lateral migration to vertical aggradation in the upper valley differs significantly from previously interpreted models of rapid flooding and transgression. Downstream the channel course becomes difficult to observe, and the stratigraphic complexity above horizon H3 increases (Figures 8, 10, 18). Rather than a single aggradational channel and associated floodplain sediments, numerous erosional unconformities, clinoforms, and dipping strata are observed (Figure 18). This transition in seismic facies potentially corresponds to the lateral transition from more fluvial or delta surface deposition to the delta front and estuarine dynamics (e.g., Aschoff et al., 2018). The latest transition from floodplain / deltaic deposition to bay and estaurine conditions is at H2, which appears to erosionally truncate the paleo-Trinity channel in the upper valley and have removed significant portions of delta stratigraphy lower in the study area (Figures 10, 11, 16, 18). This transition is associated with the appearance of potential tidal inlet complexes and a significant shift in foraminiferal abundances indicating more open or middle bay conditions (Figures 14; Rodriguez et al., 2005).

CONCLUSIONS

The succession of incised valley fill deposits located within the Trinity paleovalley broadly represents a transgressive backstepping of depositional environments. However, we find that the many of the internal changes in architecture and lithology are more likely due to changes in fluvial morphology and associated patterns of sedimentation during relative sea-level rise. In contrast to earlier work that focused on discrete flooding events driving transgression followed by periods of progradation, the paleo-fluvio to deltaic transition highlighted here appears to be more gradual and associated with a shift from lateral migration and reworking of coarse grained sediments to a period of vertical channel aggradation and enhanced fine grained floodplain and levee deposition. It is only towards the upper portion of the valley stratigraphy that evidence of significant transgression of the fluvial system is observed, and a marked transition to more bay or estuarine conditions. We find that the patterns of floodplain and delta sedimentation are closely correlated with position and geometry of the channel set during the period of channel belt growth and amalgamation, showing that rather than being a relict surface that is rapidly flooded and then deposited over it remains an active sediment routing pathway through much of the period recorded within the valley stratigraphy.

ACKNOWLEDGEMENTS

The authors would like to thank C. Speed, M. Davis, D. Duncan, G. Christeson, D. Mohrig, the members of the MG&G research group, and the crew of the R/V Manta provide Support for the author and field work was provided by a Bureau of Ocean Energy Management cooperative agreement (M16AC00020).

Figures

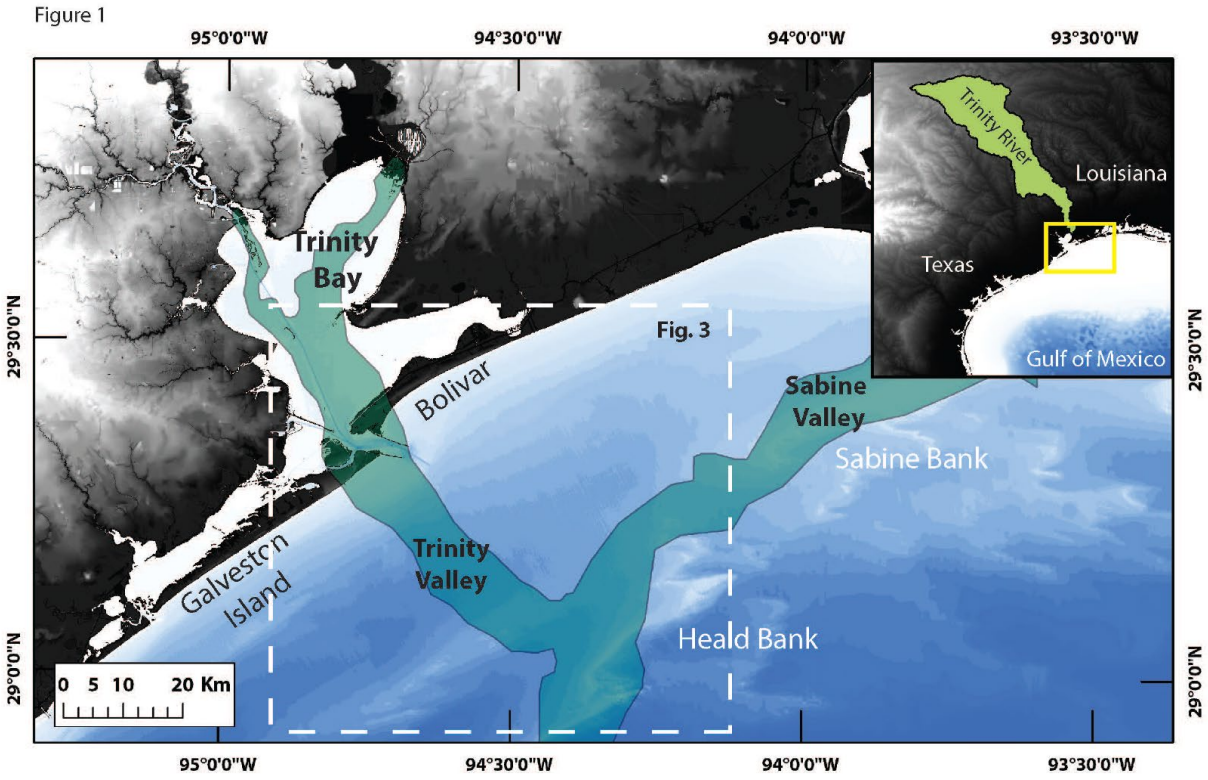

Figure 1: The east Texas inner continental shelf and Trinity incised valley

Map of the study area. The shaded valley represents the previously determined extent of the Trinity and Sabine incised valley systems during MIS2. Inset panel shows location of study area within the northern Gulf of Mexico and the outline of the modern Trinity river drainage basin. MIS2: Marine Isotope Stage 2.

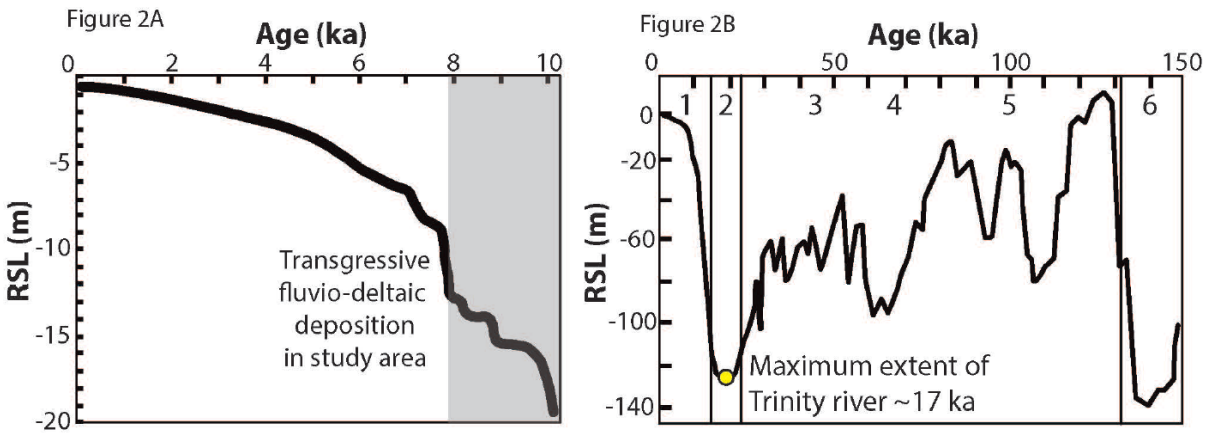

Figure 2: Holocene and last ~150 ka sea level curves

A) Composite sea level curve for the study area (modified from Milliken et al., 2008). The grey area represents the previously determined period of fluvial/deltaic sedimentation prior to transgression and onset of estuarine conditions (Anderson et al., 2016). B) Eustatic sea-level curve modified from Shackleton (2000). Marine Isotope Stages (MIS) 1-6 are labeled. The yellow dot indicates when the paleo-Trinity river reached its maximum shelf-edge location at ~17 ka (Thomas and Anderson, 1994).

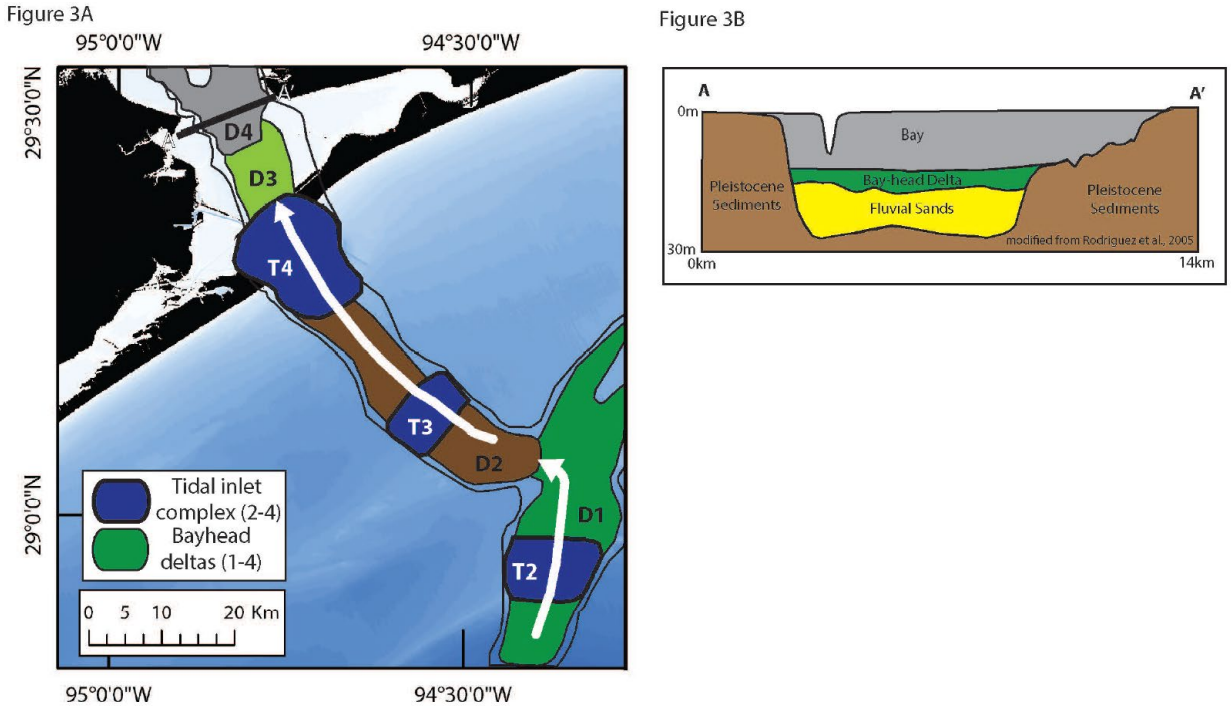

Figure 3: Transgressive depositional sequences of the Trinity valley

A) Map of backstepping bayhead deltas and associated tidal inlets infilling the Trinity incised valley during the Holocene transgression (modified from Anderson et al., 2016). The study area covers the interpreted delta 2 and tidal inlet complex 3, formed ~7-8 ka. B) Schematized cross section (A-A') showing typical stratigraphy of the incised valley fill.

Figure 4

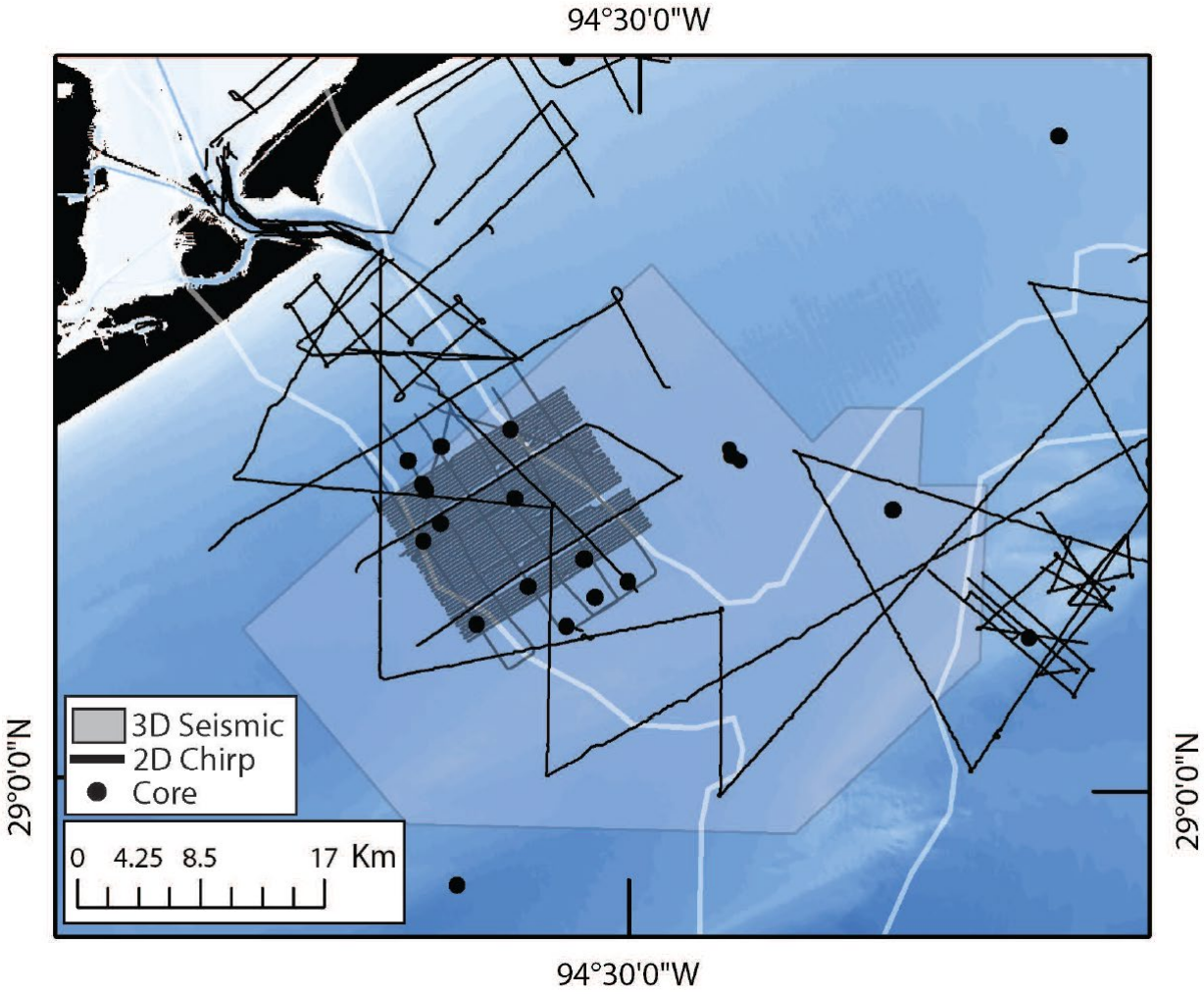

Figure 4: Data coverage of the Trinity incised valley

Map of available seismic and geologic data for the study area. Black lines represent chirp geophysical data while black dots represent cores acquired as part of this study or digitized from previous reports, literature, or archives. The grey shaded region represents the footprint of an industry 3D seismic survey.

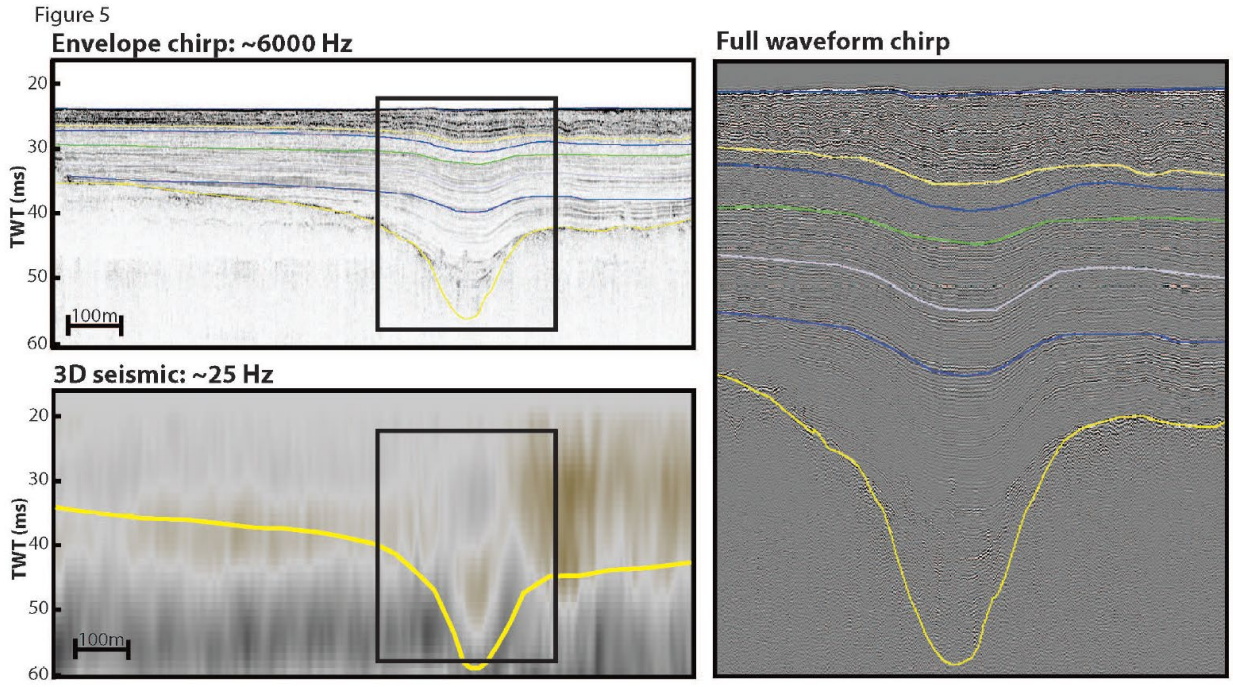

Figure 5: Comparison of seismic data types and resolutions

Comparison of envelope chirp, full waveform chirp, and 3D seismic crossline resolution for the same location. A set of arbitrary reflections are shown on chirp lines to illustrate high-resolution nature of chirp data. The same yellow horizon is shown on the chirp and 3D seismic to show the difference in vertical resolution and reflector discrimination.

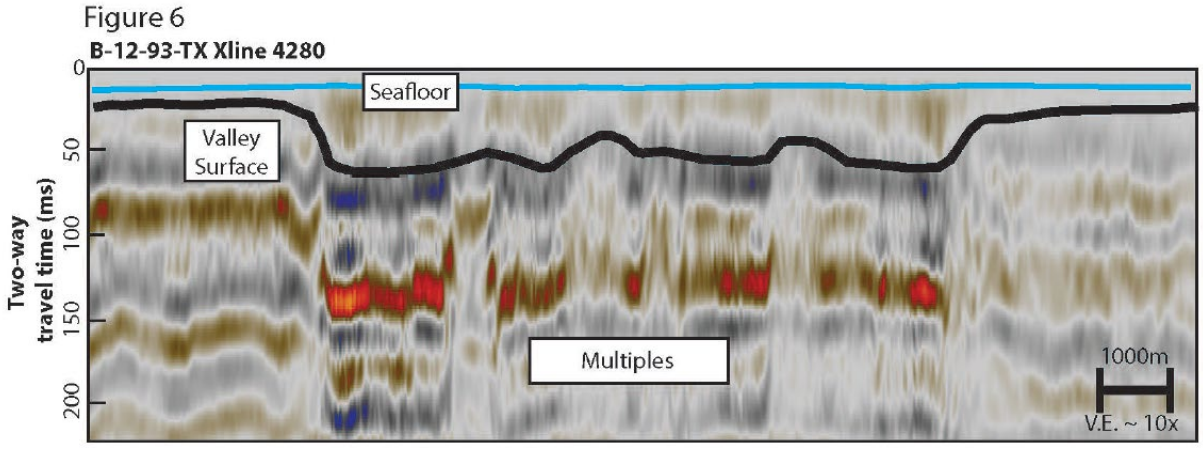

Figure 6: 3D seismic crossline of the Trinity incised valley

Example crossline from 3D seismic survey showing the appearance of the valley unconformity at ~40-65 ms. The valley surface depth was estimated from published depths as well as appearance in chirp data. Note the significant multiples and acoustic ringing below the valley compared to outside the valley.

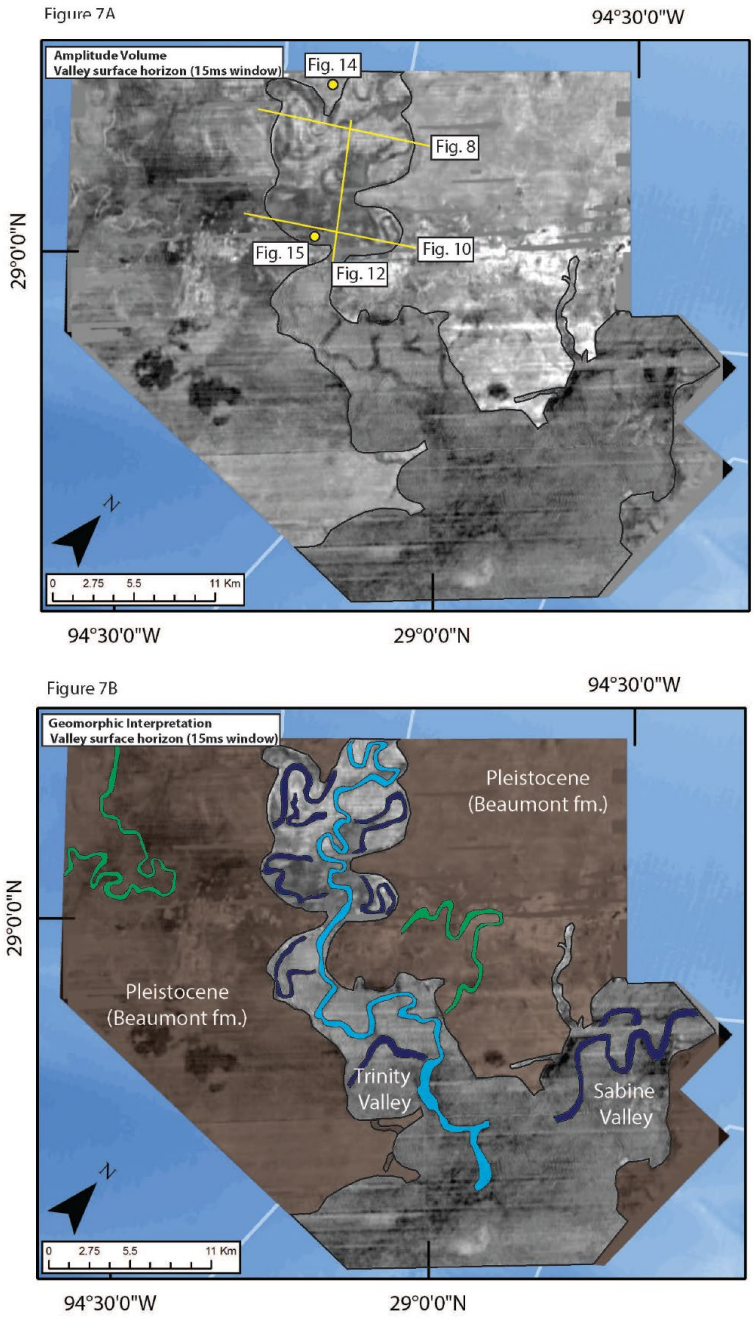

Figure 7: 3D attribute extract of valley surface horizon

A) Amplitude attribute computed for 3D seismic volume and extracted in a 20ms window along the mapped valley surface horizon. Note the appearance of multiple potential geomorphic and stratigraphic elements. as well as the chirp lines in figures 8, 10, and 12. Figures 14 and 15 are the locations of core and platform borings used to constrain depositional environment and lithology. B) Interpretation of potential morphological and structural elements present at the valley surface depth. The valley edges are well imaged, as are numerous sinuous channel forms both within and without the valley.

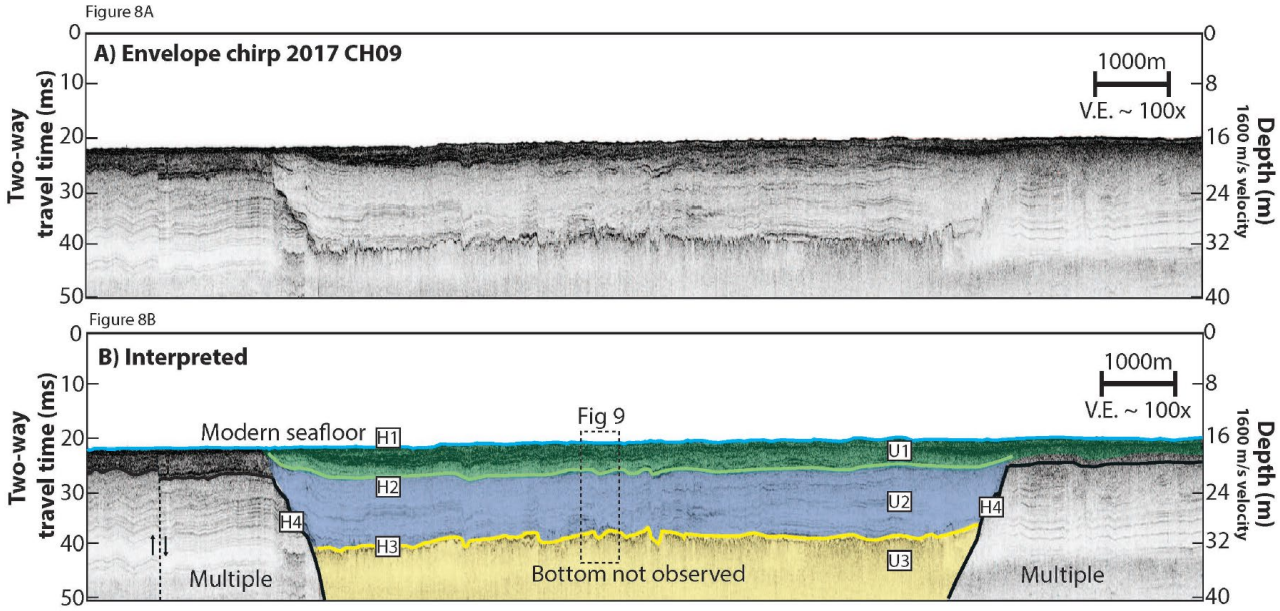

Figure 8: Chirp strike line across the valley at upper extent of study area

A) Uninterpreted envelope chirp line across the valley at 100x vertical exaggeration. B) Interpreted envelope chirp with 4 key horizons (H1-H4) shown. H1 corresponds to the modern seafloor, while H4 is the valley unconformity. Note that the base of the valley is not observed due to a combination of energy loss and acoustic blanking along the base of the valley.

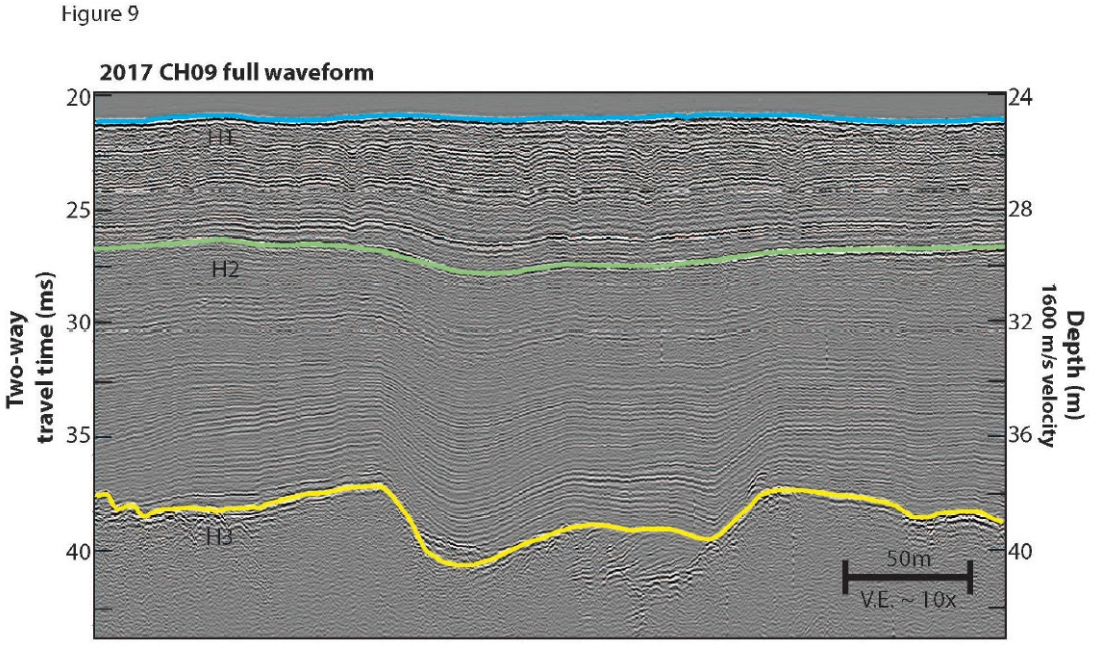

Figure 9: Example of full waveform chirp imaging of valley stratigraphy. Note the conformable, layered appearance of all layers above the basal layer H3.

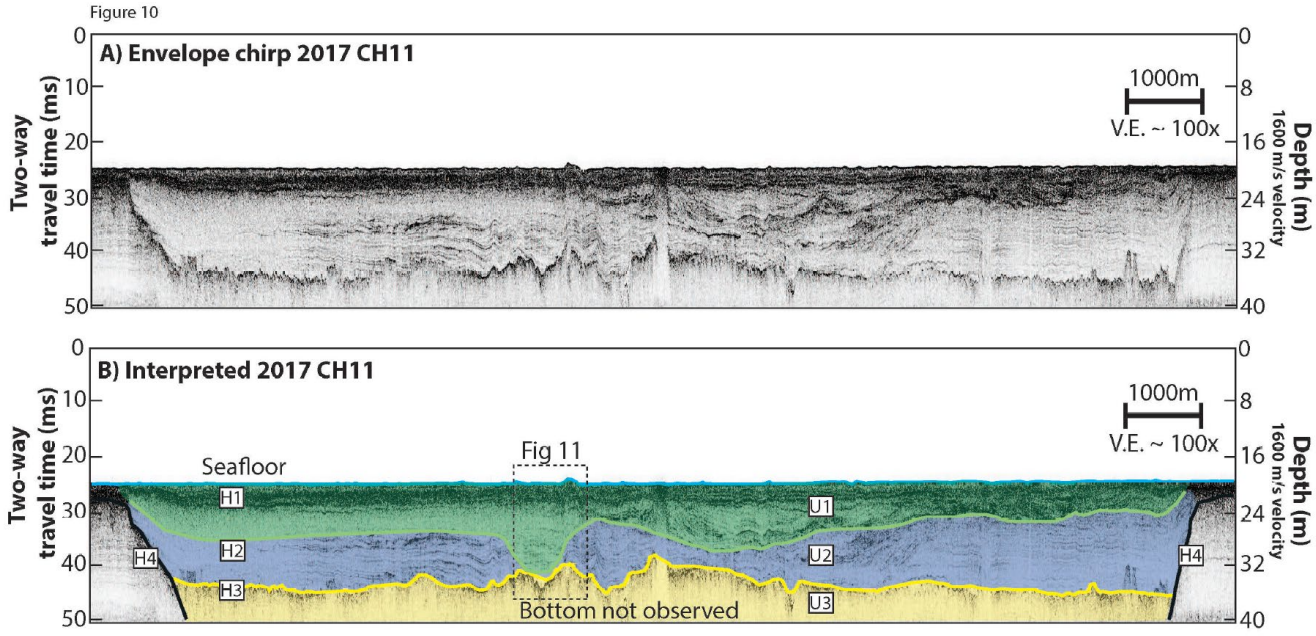

Figure 10: Chirp strike line across the valley at lower extent of study area

A) Uninterpreted envelope chirp line across the valley at 100x vertical exaggeration. B) Interpreted envelope chirp with 4 key horizons (H1-H4) shown. Note the apparent relief and unconformable nature of horizon H3 compared to further up-valley.

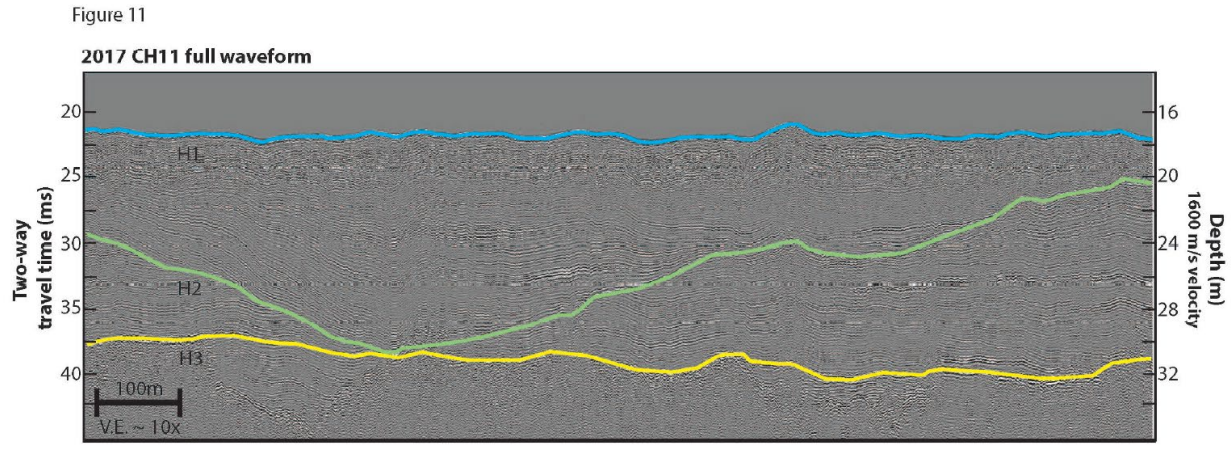

Figure 11: Example of full waveform chirp imaging of valley stratigraphy. Significant scours and erosional surfaces are observed, with truncation of H4 and other lower layers.

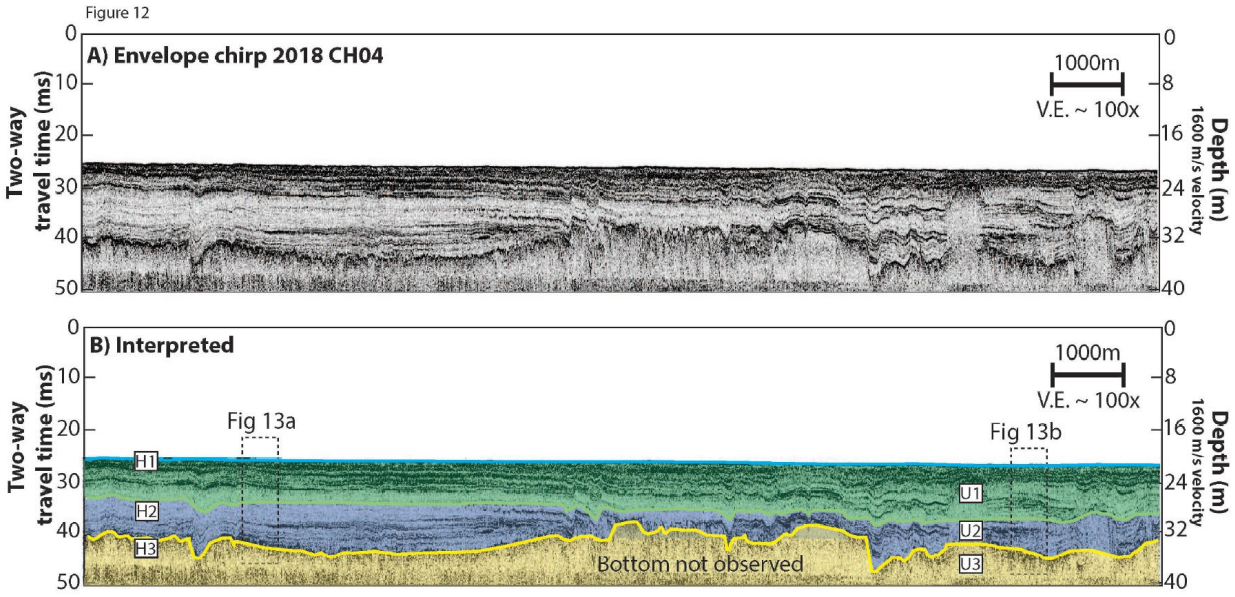

Figure 12: Chirp dip line down center of the valley

A) Uninterpreted envelope chirp down the valley axis at 100x vertical exaggeration. B) Interpreted envelope chirp with 6 key horizons (H1-H6) shown. Note the transition from conformable, sub-parallel layered stratigraphy upvalley to significant relief and erosional unconformities downvalley.

Figure 13

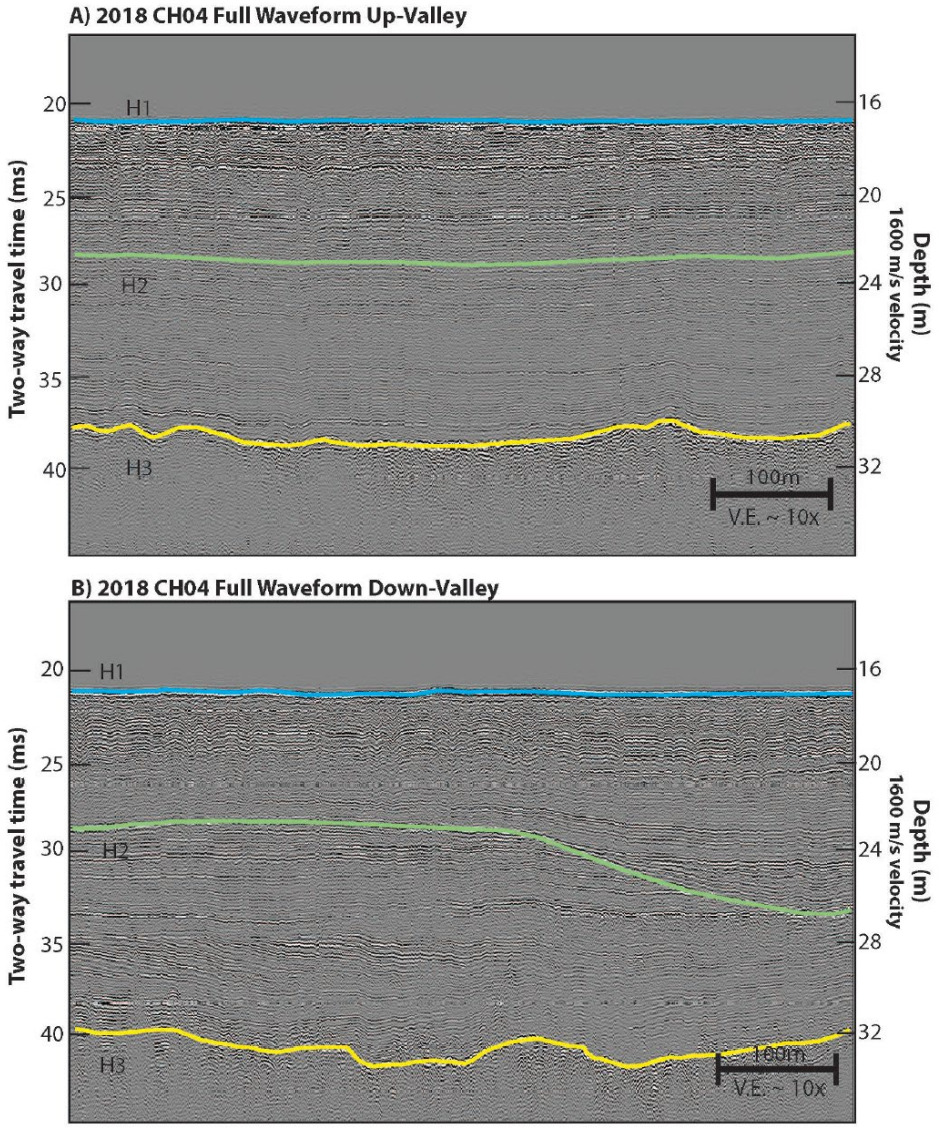

Figure 13:

A) Full waveform example of up valley stratigraphy showing conformable layers. B) Full waveform example down valley showing same horizons transitioning from conformable to unconformable and scouring out lower valley stratigraphy.

Figure 14

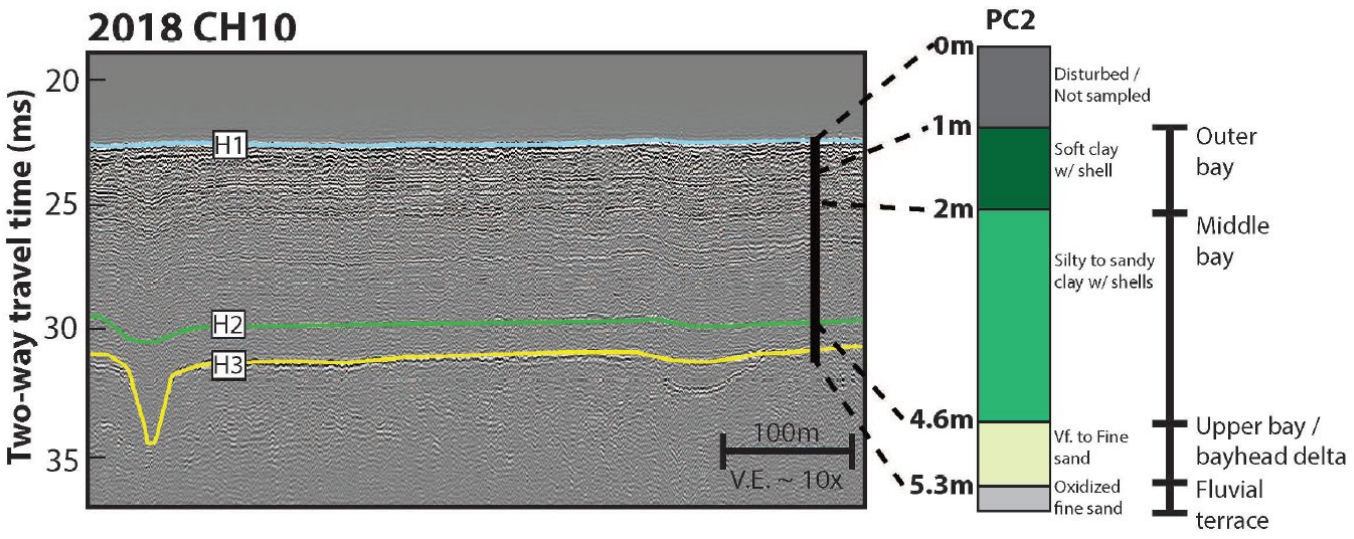

Figure 14: Core penetrating top of fluvial terrace and correlation to full waveform chirp

Piston core that penetrated the top of a fluvial terrace imaged in chirp. Paleo-environmental interpretation is based on relative abundance of foraminifera species. The majority of the core sampled H1-H2 which correlates to outer and middle bay, and a thin layer of upper bay / bay-head delta. The base of the core recovered oxidized sands with no forams, indicating terrestrial conditions.

Figure 15

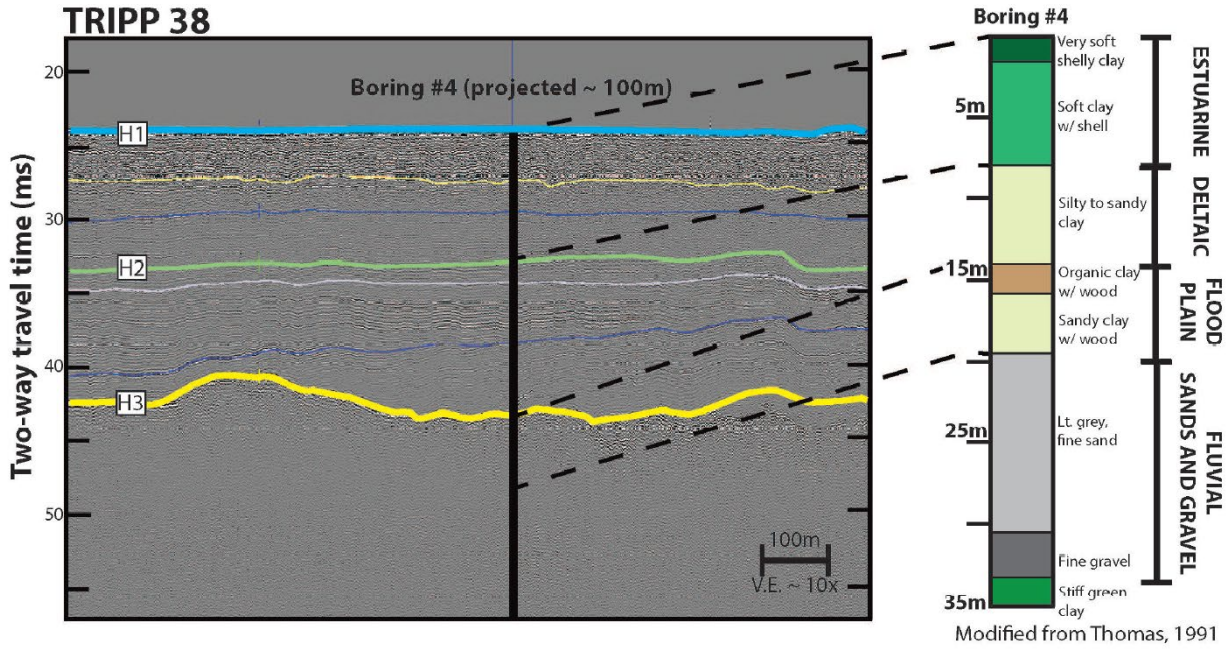

Figure 15: Paleo-environments of valley fill stratigraphy based on core- chirp correlation

Platform boring that penetrated entire Trinity valley stratigraphy. Lithology and interpreted environment from Thomas (1991) with correlation to mapped horizons. H2 correlates with the transition to estuarine from deltaic conditions. H3, or the top of the acoustically impenetrable package, correlates with the top of the floodplain/fluvial sediments.

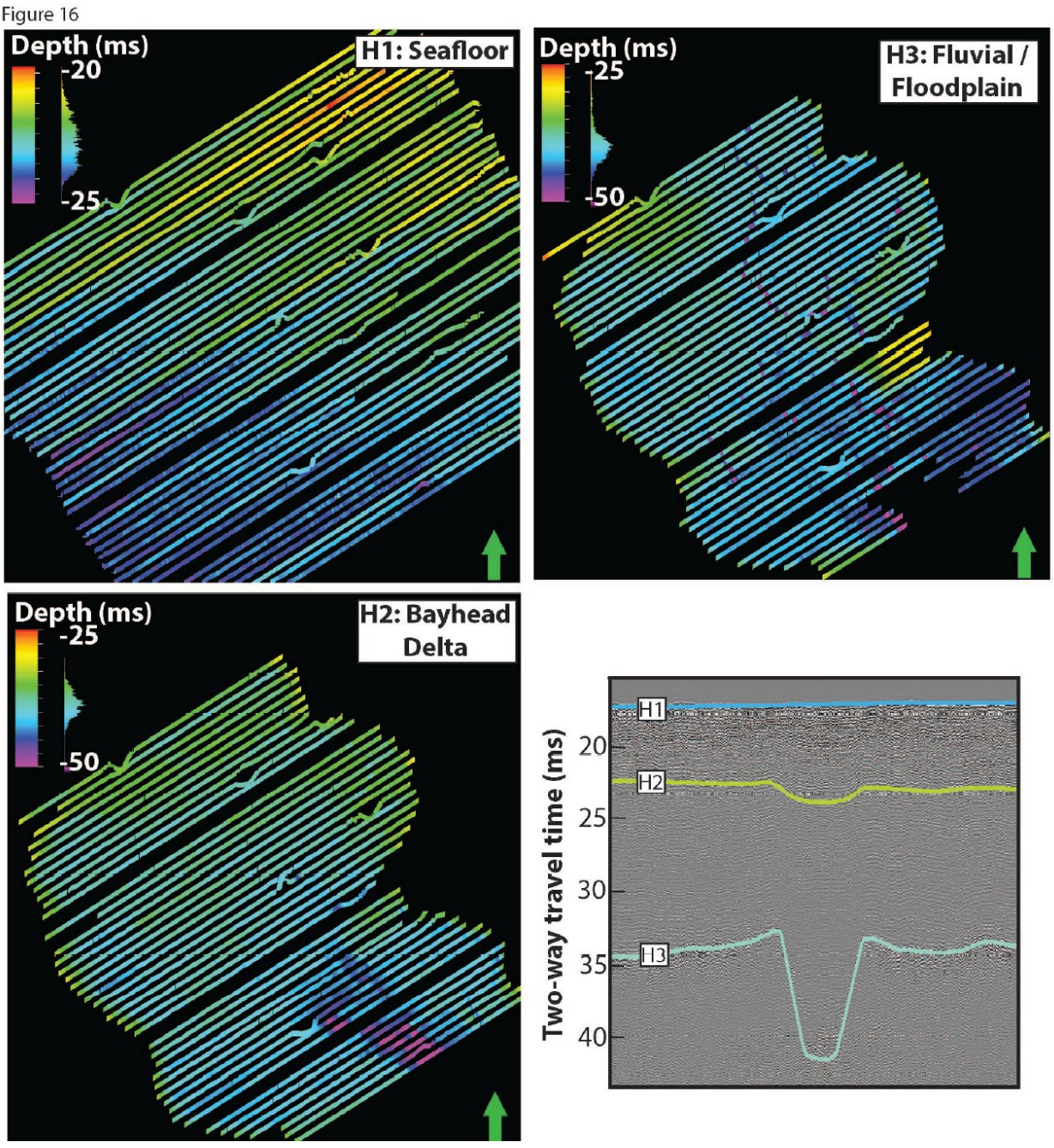

Figure 16: Time structure maps of key horizons and example full waveform chirp line

Time-structure mapping of H1, 2, and 3. Horizons are not interpolated between lines to preserve fine-scale details. Warm colors correspond to shallow depths, while cool colors are deeper. Paleo-environmental interpretations from Thomas and Anderson (1994) and this study. A) H1, or the modern seafloor. B) H2, or bayhead delta / upper bay. C) H3, or fluvial /floodplain. Note the appearance of numerous narrow, deep segments that form sinuous channel courses. D) Example full-waveform chirp line illustrating mapped horizons H1, 2, and 3.

Figure 17

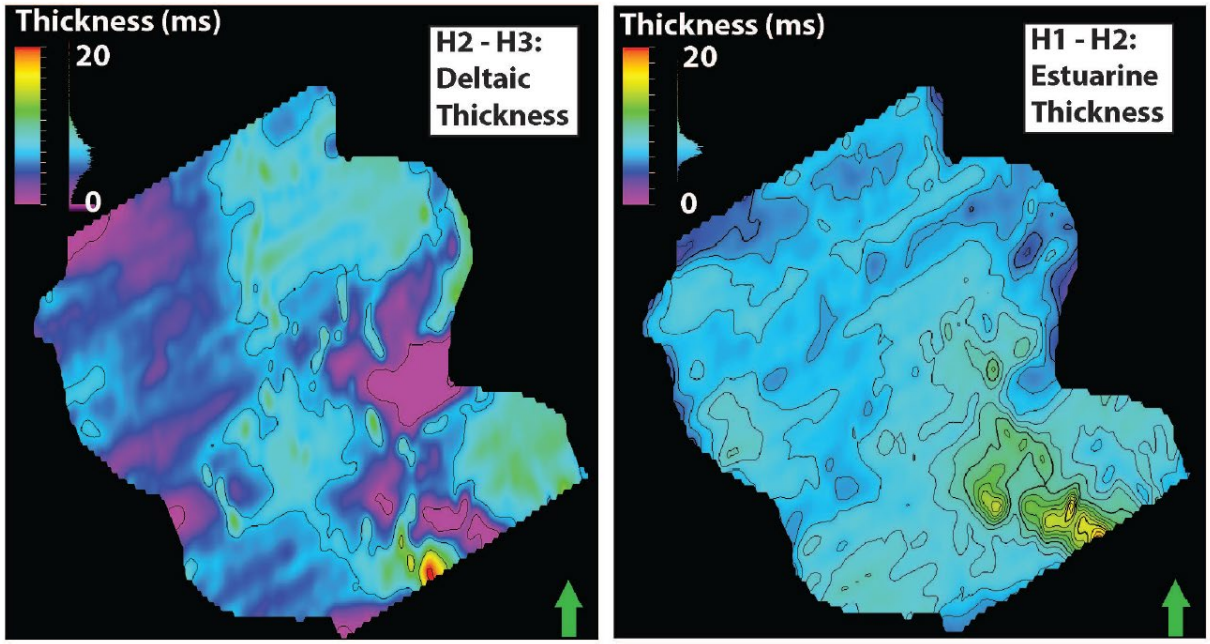

Figure 17: Thickness maps (ms) of Trinity valley stratigraphy

Time-thickness maps of key stratigraphic intervals. Warm colors correspond to shallow depths are thicker, while cool colors are deeper. A) Thickness of the estuarine (H1-H2), or U1, package. B) Thickness of the deltaic (H2-H3), or U2, package.

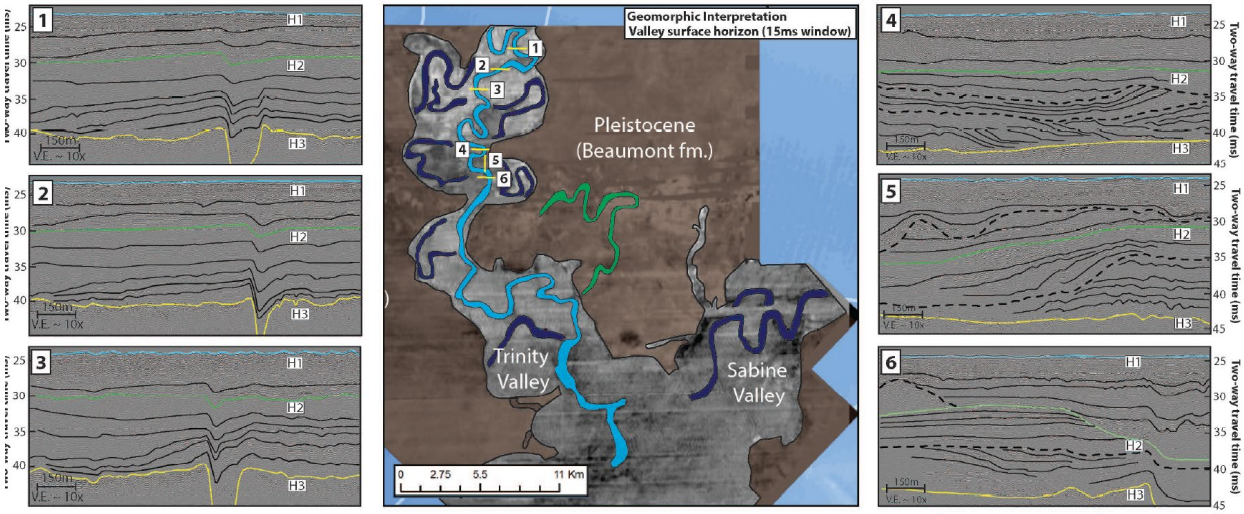

Figure 18: Chirp lines crossing paleo-Trinity channel

Representative chirp cross sections across the interpreted paleo-Trinity channel. Cross sections 1-3 illustrate vertical channel aggradation and associated horizon downlap on H3 (floodplain). Cross sections 4-6 show lower valley stratigraphy previously interpreted as deltaic comprised of numerous progradational clinoforms, scour surfaces, and sigmoidal depositional packages. Paleo-channel forms in association with H3 not commonly observed

References

Aschoff, J.L., Olariu, C., Steel., R.J., 2018. Recognition and significance of bayhead delta deposits in the rock record: A comparison of modern and ancient systems. Sedimentology 65, 62-95.

Anderson, J. B., A. B. Rodriguez, K. Milliken, and M. Taviani (2008), The Holocene evolution of the Galveston estuary complex, Texas: Evidence for rapid change in estuarine environments, in Response of Upper Gulf Coast Estuaries to Holocene Climate Change and Sea-Level Rise, Geol. Soc. of Am. Spec. Pap. 443, edited by J. B. Anderson and A. B. Rodriguez, pp. 89–104

Burstein, J., Goff, J. A., Gulick, S., Lowery, C., Standring, P., & Swartz, J. (2021). Tracking Barrier Island Response to Early Holocene Sea-level Rise: High Resolution Study of Estuarine Sediments in the Trinity River Paleovalley.

Blum, M.D., and Tornqvist, T. (2000). Fluvial response to climate and sea-level change: a review and look forward: Sedimentology, 47, pp.2-48

Blum, M.D., Martin, J.M., Milliken, K.T., and Garvin, M. (2013). Paleovalley systems: Insights from Quaternary analogs and experimental studies: EarthScience Reviews, v. 116

Calves, G., Huuse, M., Schwab, A., Clift, P., 2008. Three-dimensional seismic analysis of high-amplitude anomalies in the shallow subsurface of the Northern Indus Fan: Sedimentary and/or fluid origin. J. Geophys. Res. 113, B11103,

Chatanantavet, P., Lamb, M.P., and Nittrouer, J.A. (2012). Backwater controls of avulsion location on deltas: Geophysical Research Letters, v. 39

Gibling, M.R. (2006). Width and thickness of fluvial channel bodies and valley fills in the geological record: A literature compilation and classification: Journal of Sedimentary Research, v. 76, p. 731–770

Hudson, P.F., and Kesel, R.H. (2000). Channel migration and meander-bend curvature in the lower Mississippi River prior to major human modification: Geology, v. 28, p. 531–534

Fernandes, A.M., Tornqvist, T.E., Straub, K.M., Mohrig, D., 2016. Connecting the backwater hydraulics of coastal rivers to fluvio-deltaic sedimentology and stratigraphy. Geology 44, 979-982.

Garcia-Gil, S., Vilas, F., Garcia-Garcia, A., 2002. Shallow gas features in incised-valley fills (Ría de Vigo, NW Spain): a case study. Cont. Shelf Res. 22, 2303-2315.

Hoyal, D. Sheets, B.A., 2009. Morphodynamic evolution of experimental cohesive deltas. J. Geophys. Res. 114, F02009.

Jerolmack, D. J. (2009). Conceptual framework for assessing the response of delta channel networks to Holocene sea level rise. Quaternary Science Reviews, 28(17), 1786–1800.

Jerolmack, D.J., and Swenson, J.B. (2007). Scaling relationships and evolution of distributary networks on wave-influenced deltas: Geophysical Research Letters, v. 34

Karssenberg, D., and Bridge, J.S. (2008). A three-dimensional model of sediment transport, erosion, and deposition within a network of channel belts, floodplain and hill slope: Intrinsic and extrinsic controls on floodplain dynamics and alluvial architecture: Sedimentology, v. 55, p. 1717–1745

Lamb, M.P., Nittrouer, J.A., Mohrig, D., and Shaw, J. (2012). Backwater and river plume controls on scour upstream of river mouths: Implications for fluviodeltaic morphodynamics: Journal of Geophysical Research, v. 117

Lentsch, N., Finotello, A., & Paola, C. (2018). Reduction of deltaic channel mobility by tidal action under rising relative sea level. Geology, 46(7), 599

Leopold, L.B., Bull, W.B., 1979. Base level, aggradation, and grade. Proc. Amer. Phil. Soc. 123, 168-202.

Mackin, J.H., 1948. Concept of the graded river, GSA Bull. 59, 463-512.

Martin, J., Sheets, B., Paola, C., & Hoyal, D. (2009). Influence of steady base-level rise on channel mobility, shoreline migration, and scaling properties of a cohesive experimental delta. Journal of Geophysical Research, 114

Mason, J., and Mohrig, D. (2018). Using time-lapse lidar to quantify river bend evolution on the meandering coastal Trinity River, Texas, USA: Journal of Geophysical Research: Earth Surface, v. 123, p. 1133– 1144

Miall, A. 2014. Fluvial Depositional Systems. Springer, New York, 316 pp.

Milliken, K. T., J. B. Anderson, and A. B. Rodriguez (2008), A new composite Holocene sea-level curve for the northern Gulf of Mexico, in Response of Upper Gulf Coast Estuaries to Holocene Climate Change and Sea-Level Rise, Geol. Soc. of Am. Spec. Pap. 443, edited by J. B. Anderson and A. B. Rodriguez, pp. 1–11

Moodie, A. J., Nittrouer, J. A., Ma, H., Carlson, B. N., Chadwick, A. J., Lamb, M. P., Parker, G., 2019. Modeling deltaic lobe-building cycles and channel avulsions for the Yellow River Delta, China. J. Geophys. Res. Earth Surf. 124, 2438– 2462.

Moran, K. E., Nittrouer, J. A., Perillo, M. M., Lorenzo-Trueba, J., & Anderson, J. B. (2017). Morphodynamic modeling of fluvial channel fill and avulsion time scales during early Holocene transgression, as substantiated by the incised valley stratigraphy of the Trinity River, Texas. Journal of Geophysical Research: Earth Surface, 122, 215–234.

Morton, R.A., Blum, M.D., and White, W.A. (1996). Valley fills of incised coastal plain rivers: Gulf Coast Association of Geological Societies, Transactions, v. 46, p. 321–331.

Nittrouer, J.A., Shaw, J., Lamb, M.P., and Mohrig, D. (2012). Spatial and temporal trends for water-flow velocity and bed-material sediment transport in the lower Mississippi River: Geological Society of America Bulletin, v. 124, p. 400–414

Simms, A. R., J. B. Anderson, K. T. Milliken, Z. P. Taha, and J. S. Wellner (2007), Geomorphology and age of the oxygen isotope stage 2 (last lowstand) sequence boundary on the northwestern Gulf of Mexico continental shelf, in Seismic Geomorphology: Applications to Hydrocarbon Exploration and Production, Spec. Publ. 277, edited by R. J. Davies et al., pp. 29–46

Shawler, J.L., Connel, J.E., Boggs, B.Q., Hein, C.J., 2020. Relative influence of antecedent topography and sea-level rise on barrier-island migration: Sediment Core Data. W&M ScholarWorks, DOI: 10.25773/8wx5-zq69.

Smith, V.B., Mohrig, D., 2017. Geomorphic signature of a dammed Sandy River: The lower Trinity River downstream of Livingston Dam in Texas, USA. Geomorphology 297, 122-136.

Sutherland, M.D., Dafforn, K.A., Scanes, P., Potts, J., Simpson, S.L., Sim, V.X.Y., Johnston, E.L., 2017. Links between contaminant hotspots in low flow estuarine systems and altered sediment biogeochemical processes. Estuar. Coast. Shelf Sci. 198, 497-507.

Standring, P., Lowery, C., Burstein, J., Swartz, J., Goff, J. A., & Gulick, S. (2021). Foraminiferal Analysis of Holocene Sea Level Rise within Trinity River Incised Paleo-Valley, Offshore Galveston Bay, Texas.

Thomas, M.A. (1991) The impact of long-term and short-term sea-level changes on the evolution of the Wisconsin–Holocene Trinity/Sabine incised-valley system, Texas continental shelf [unpublished Ph.D. dissertation]: Rice University, Houston, 247 p.

Thomas, M. A., and J. B. Anderson (1994), Sea-level controls on the facies architeture of the Trinity/Sabine incised-valley system, Texas continental shelf, in Incised-Valley Systems: Origin and Sedimentary Sequences, SEPM Spec. Publ. 51, edited by R. W. Dalrymple, R. Boyd, and B. A. Zaitlin, pp. 63–82, SEPM, Tulsa, Okla.

Torres, M.A., Limaye, A.B., Ganti, V., Lamb, M.P., West, A.J., Fischer, W.W., 2017. Model predictions of long-lived storage of organic carbon in river deposits. Earth Surf. Dynam. 5, 711-730.

Trower, E.J., Ganti, V., Fischer, W.W., Lamb, M.P., 2018. Erosional surfaces in the Upper Cretaceous Castlegate Sandstone (Utah, USA): Sequence boundaries or autogenic scour from backwater hydrodynamics? Geology 46, 707-710.

Van Wagoner, J.C., Mitchum, R..M., Campion, K.M., Rahmanian, V.D.,1990. Siliciclastic sequence stratigraphy in well logs, cores, and outcrops: Concepts for high-resolution Ccorrelation of time and facies. AAPG Methods in Exploration Series, No. 7., 1-55.

Zaitlin, B.A., Dalrymple, R.W., and Boyd, R. (1994). The stratigraphic organization of incisedvalley systems associated with relative sea-level change, in Dalrymple, R.W., Boyd, R., and Zaitlin, B.A., eds., Incised Valley Systems: Origin and Sedimentary Sequences: SEPM, Special Publication 51, p. 45–60.

Zheng, S., Edmonds, D. A., Wu, B., & Han, S. (2019). Backwater controls on the evolution and avulsion of the Qingshuigou channel on the Yellow River delta. *Geomorphology*, 333, 137–151.

1.